VNU Journal of Science: Mathematics – Physics, Vol. 40, No. 1 (2024) 61-72

VNU Journal of Science: Mathematics - Physics

Journal homepage: https://js.vnu.edu.vn/MaP

Original Article

Binder Parameter in a Generalized Two-dimensional XY Model

Duong Xuan Nui[1,3], Truong Thi Bach Yen[2], Nguyen Huu Cuong[3], Luu Bich Linh[3], Bui Thi Toan Thu[3], Nguyen Vu Cam Binh[3], Nguyen Thi Huyen[3], Nguyen Ngoc Anh[4], Dao Xuan Viet[1,*]

[1]*International Training Institute for Materials Science, Hanoi University of Science and Technology, 1 Dai Co Viet, Hai Ba Trung, Hanoi, Vietnam*

[2]*Dong Thap University, 783 Pham Huu Lau, Ward 6, Cao Lanh City, Dong Thap, Vietnam*

[3]*Vietnam National University of Forestry, National Road 21, Xuan Mai, Chuong My, Hanoi, Vietnam*

[4]*Hanoi University of Industry, 298 Cau Dien, Bac Tu Liem, Hanoi, Vietnam*

Received 11 August 2023
Revised 30 August 2023; Accepted 18 March 2024

Abstract: We performed Monte Carlo simulation for a two-dimensional generalized XY model and calculated the magnetic and nematic Binder parameters. The phase diagram is re-examined based on these Binder parameters, demonstrating their power in studying generalized XY models. The Binder parameter has distinctive behaviors, resulting in different types of phase transition. More importantly, the magnetic Binder parameter gives more insights into the tricritical region where the Kosterlitz-Thouless, Ising, and 1/2 Kosterlitz-Thouless (KT) transition lines meet. It shows signatures for the intermediate region starting from the tricritical point, where the transition line is neither the same physics as the Ising transition below nor the KT transition far above the tricritical point.

Keywords: Monte Carlo simulations, phase transitions, magnetic materials.

1. Introduction

The Mermin-Wagner theorem states that in two dimensions, continuous symmetry breaking cannot occur at finite temperatures for systems with short-range interactions [1]. A two-dimensional XY model is particular because it exhibits a different type of phase transition known as the Kosterlitz-Thouless

* Corresponding author.
E-mail address: viet.daoxuan@hust.edu.vn

https//doi.org/10.25073/2588-1124/vnumap.4868

(KT) transition, associated with unbinding vortices and antivortices. In high temperatures, the vortices and antivortices are free, and the system is in a disordered phase, where the spinspin correlation function decays exponentially. As the temperature decreases, vortices and antivortices form bound pairs, and the system undergoes the KT transition. In the low-temperature phase, these bound vortexantivortex pairs lead to quasi-long-range order, where the spin-spin correlation function decays algebraically [2, 3].

The generalized XY models [4, 5], which include nematic effects, have gained much attention because of their possibility for investigating KT phase transitions in liquid crystal [5, 6] or in He3 thin films [4, 7, 8]. The generalized XY models include additional nematic interactions to the original magnetic interaction. In addition to the conventional vortices and antivortices generated by the magnetic interaction, the system exhibits 1/q-integer vortices. The interplay between integer and noninteger vortices can lead to rich phase diagrams and transitions.

The relative strengths of the magnetic and nematic interactions in the generalized XY model experience the nature of phase transitions. When the magnetic interaction is dominant, it behaves like the conventional XY model with a KT transition from a disordered paramagnetic phase to a quasi-long-range ordered phase characterized by the binding of vortex-antivortex pairs. In contrast, if the nematic interaction is dominant, a nematic phase can be stable at low temperatures with bound pairs of noninteger vortices. When both interactions contribute, there are three possible phases in the phase diagrams that meet at a tricritical point: the disordered (paramagnetic) phase (P), the quasi-long-range ordered phase (F), and the nematic phase (N) [4, 5, 9-12]. Away from the multicritical region, the phase transitions from the disordered to the nematic or the quasi-long-range phase belong to the KT universality class [9, 13], while the transition from the nematic to the quasi-long-range order belongs to the Ising university class [10, 12].

The phase diagram of the generalized 2D XY model has been constructed since the early days of the model [4, 5, 9], and much of its critical behavior is relatively well understood. One of the remaining issues is whether the tricritical point is an actual tricritical point where all the phase boundaries meet or if there are segments of phase boundaries that extend beyond the tricritical point. Recent works have suggested that the Ising line, corresponding to the transition from the nematic to the quasi-long-range ordered phase, can extend beyond the tricritical point [13-15]. It means a segment of the phase boundary where the transition directly from the quasilong-range phase to the disordered phase belongs to the Ising universality class. Reference 15 regarded it as a classic example of the deconfined quantum criticality [16]. Most recent works have suggested that the Ising phase transition terminates at the tricritical point, leading to an intermediate region between the Ising and KT lines. This intermediate region is of a distinct type of phase transition that differs from both the Ising and KT transitions [17, 18].

In this work, we employed large-scale Monte Carlo simulations and focused on measuring the Binder parameters. This quantity has been investigated for various models [19-22] and the generalized 2D XY model with $q > 2$ [10]. However, it has yet to be studied rigorously for the generalized XY model with $q = 2$. By conducting a detailed analysis of the magnetic and nematic Binder parameters, we have reproduced the phase diagram of the generalized XY model. Moreover, these measurements of the Binder parameters support more insights into the physics of the tricritical region, particularly concerning the understanding of the Ising phase boundary that originates from the N-F transition, how this boundary ends, and how the system changes from the Ising transition line to the KT transition line as the relative strengths of the interactions are varied.

2. Model and Methods

The Hamiltonian of the two-dimensional generalized XY model with both magnetic and 2-nematic interactions is as follows.

$$H = -\sum_{<ij>}\Big[\Delta cos(\theta_i - \theta_j) + (1-\Delta)cos(2\theta_i - 2\theta_j)\Big], \quad (1)$$

where θ_i (θ_j) are the angles of the spin orientations at sites $i(j)$. $\langle ij\rangle$ denotes the sum over nearest-neighbor pairs of spins. Δ is the strength of the magnetic interaction with the unit energy scale setting 1. $1-\Delta$ is the strength of the 2-nematic interaction. The relative strength of the two interactions by tuning the parameter Δ from 0 to 1.

We simulate the two-dimensional generalized XY model on a square lattice with periodic boundary conditions using Monte Carlo method. The lattice size L ranges from 16 to 256. We measure physical quantities in the thermodynamic limit and then extrapolate the data from simulations with various sizes of L.

The Monte Carlo simulation uses two types of updates: local single-spin-flip Metropolis algorithm and clusterspin-flip algorithm following the Wolff algorithm [23]. Local and cluster updates are carried out once in every Monte Carlo step. The Monte Carlo simulation parameters for each case are summarized in Table 1. To ensure that the system is in equilibrium by checking the quality of the specific heat computed via energy fluctuation and the specific heat calculated via the temperature difference of the energy.

Table 1. Various simulation parameters are listed here. L is the system size, N_r is the number of the independent run, N_{MC} is the total number of MC steps, and N_T is the total number of temperature points

Δ	L	N_r	N_{MC}	N_T	Δ	L	N_r	N_{MC}	N_T
0.2	16	5	8.10^6	63	0.4	16	5	8.10^6	63
	32	5	8.10^6	63		32	5	8.10^6	63
	64	5	8.10^6	63		64	5	8.10^6	63
	128	5	10.10^6	55		128	5	10.10^6	63
	256	5	12.10^6	26		256	5	12.10^6	25
0.3	16	5	8.10^6	63	0.7	16	5	8.10^6	63
	32	5	8.10^6	63		32	5	8.10^6	63
	64	5	8.10^6	63		64	5	8.10^6	63
	128	5	10.10^6	55		128	5	10.10^6	63
	256	5	12.10^6	27					
0.36	16	5	8.10^6	63					
	32	5	8.10^6	63					
	64	5	8.10^6	63					
	128	5	10.10^6	63					
	256	5	12.10^6	27					

The magnetization (m_1) and the nematic magnetization (m_2) are defined as [23]

$$m_n = \frac{1}{N}\sqrt{\left(\sum_{i=1}^{N} cos(n\theta_i)\right)^2 + \left(\sum_{i=1}^{N} sin(n\theta_i)\right)^2}, \quad (2)$$

The magnetic Binder parameter (g_1) and the nematic Binder parameter (g_2) are defined as [19-21, 24].

$$g_n = 2 - \frac{\langle m_n^4 \rangle}{\langle m_n^2 \rangle}, \quad (3)$$

where < ... > denotes thermal average, m1 is the magnetic magnetization, and m2 is the nematic magnetization. For the 2D Ising model, the Binder ratio shows a crossing behavior at the second-order phase transition. On the other hand, for the 2D XY model, the Binder ratio shows a merging behavior at the KT phase transition [21].

A similar definition of the difference of correlation length [17], we define the difference of the magnetic Binder parameter at different L values (δ_{g1}) as follows.

$$\delta_g(L) = \frac{g_1(2L)}{2L} - \frac{g_1(L)}{L}, \tag{4}$$

3. Phase Diagram

We reproduce the phase diagram of the generalized 2D XY model at $q = 2$ [Eq. (1)] using the Binder parameters to demonstrate the power of these quantities for studying spin models. Binder parameters have two distinctive behaviors when the temperature crosses the critical value. In detail, when plotting $g(L)$ for different L's, they either merge below the critical temperature or cross each other at the critical point. From these behaviors, we determine the critical temperature and understand the nature of the phase transition. The Binder parameter is the accurate method for locating phase transitions and plays a crucial role in revealing the physics of the phase transitions.

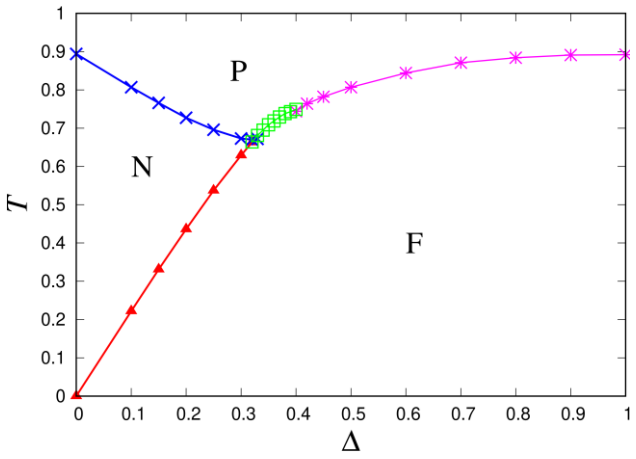

Figure 1. The $T-\Delta$ phase diagram for the 2D generalized XY model at $q = 2$ is reconstructed using the Binder parameters. The diagram displays three distinct phases: disordered (P), nematic (N), and quasi-long-range ferromagnetic (F) phases. The yellow square thick line represents the phase boundary that is the focus of this study. The green square line is obtained based on the nematic Binder parameter. The intersection of these two lines determines the tricritical point Δ_c. The P → N green square and the P → F blue dot lines belong to the KT universality class; the N → F purple triangle line belongs to the Ising universality class, while the nature of the P → F yellow square line is under investigation. The error bars are smaller than the symbol sizes.

We represent in Figure 1 the $T-\Delta$ phase diagram of the model, here T is the normalized temperature. The phase diagram clearly shows three distinct phases: i) The disordered phase (P); ii) The quasi-longrange ordered phase (F), and iii) The nematic phase (N). Different behaviors of the magnetic and nematic Binder parameters characterize these phases. The three phase boundaries meet at one point, the tricritical point $\Delta_c \approx 0.325$. The result is consistent for the locations of the phases as well as the existence

of the tricritical point with previous Monte Carlo studies, which constructed the phase diagram using other physical measurements such as the specific heat and the magnetic susceptibility [9] or the helicity modulus [13] or the correlation length [17].

In the region of small Δ (Δ< Δ_c), the nematic interaction plays an important role. The two-phase transitions: i) The P → N KT transition at a high temperature which is related to the binding and unbinding of 1/2-vortices; and ii) The N → F Ising transition at a low temperature occurred when the string tension between 1/2-vortices vanishes [13].

c2a shows the magnetic Binder parameter at Δ = 0.2. The magnetic Binder curves g_1 cross nearly the same point at $T \approx 0.436$, analogous to the Binder parameter behavior in the 2D Ising model. The crossing behavior of the magnetic Binder parameter indicates an Ising phase transition. One more, the magnetic Binder parameter rapidly changes at $T \approx 0.436$ from positive to negative value, indicating a transition to a phase with nontrivial winding configurations. Therefore, in this generalized XY model, the behavior of the magnetic Binder parameter suggests an Ising-like phase transition from the quasi-long-range ordered phase to the nematic phase, which is different from that of the Ising model, where it is from the long-range ferromagnetic order to the paramagnetic phase.

We specify the crossing temperature $T_c(L)$ for each pair of L and $2L$ to estimate the phase transition temperature. Then, the critical temperature T_c is obtained by fitting $T_c(L)$ following Eq. (5), we obtain $T_1 = 0.436$ for this Δ. It is consistent with previous studies [9, 13, 17].

$$T_c(L) = T_c + a.L^{-1/\nu}, \tag{5}$$

On the other hand, the behavior of the magnetic Binder parameter at higher temperatures ($T > 0.436$) shows exciting features. It rapidly decreases from a positive to a negative value at $T \approx 0.436$, slightly increases in the temperature range 0.436 to 0.78, and then rapidly increases to zero at $T \approx 0.78$. The rapid decrease of the magnetic Binder parameter from a positive to a negative value suggests a possible transition at $T = 0.436$ to a phase with non-trivial winding configurations. The subsequent increase of the Binder parameter to zero at $T = 0.78$ indicates a signature of another transition from this non-trivial winding phase to the disordered phase. This phase transition will determine clearly from the nematic Binder parameter in the next.

The temperature dependence of the nematic Binder parameter is present in Figure 2b. The g_2 curves of different system sizes (L) merge at $T \approx 0.8$ further confirms the presence of a KT phase transition (from the nematic phase (N) to the disordered phase (P)), which is governed by the binding and unbinding of half-vortices. This behavior is similar to the transition observed in the conventional XY model, where the KT phase transition is also associated with the binding and unbinding of vortices and antivortices [21].

We apply the method from Ref. [25] for determining the KT phase transition. It is challenging to locate the merging point for g_2 at different L's. Instead, we choose a value R smaller but not too far from the critical value of g_2 such that $g_2(T) = R$ has a solution $T_c(L)$ larger than T_c. To extrapolate T_c in the limit $L \to \infty$ following Eq. (6), we obtained a critical temperature of $T_2 \approx 0.727$ for this KT transition. It is consistent with previous work of the generalized XY model [4, 5, 13, 17].

$$T_c(L) = T_c + \frac{c^2 T_c}{(\ln bL)^2}. \tag{6}$$

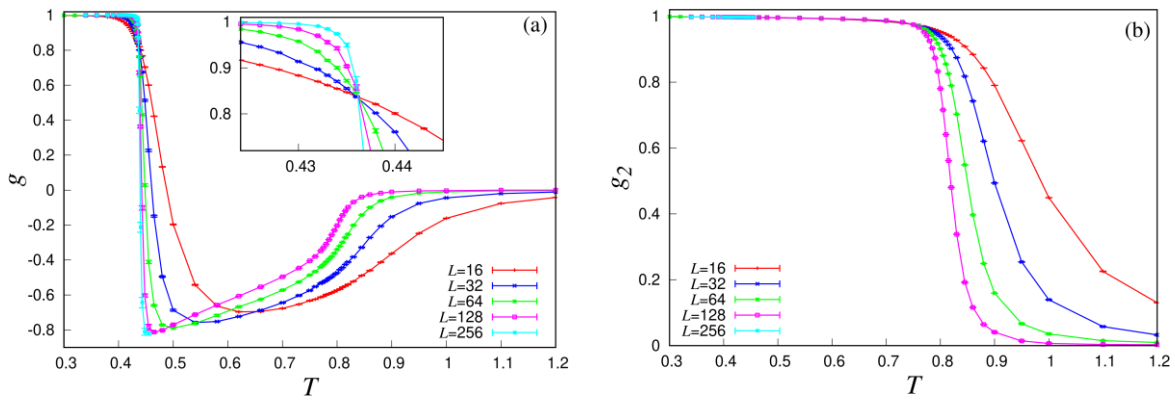

Figure 2. Temperature dependence of the magnetic Binder parameter g1 (a) and the nematic Binder parameter g2 (b) for Δ = 0.2. The inset in panel (a) is the expanded view of the magnetic Binder parameter around the crossing temperature. The error bars are smaller than the symbol sizes.

In the region of large Δ (Δ > 0.4), the magnetic interaction dominates over the 2-fold nematic interaction, leading the system to resemble the conventional 2D XY model. Figure 3 shows the temperature dependence of the magnetic (g_1) and nematic (g_2) Binder parameter for Δ = 0.7. At low temperatures, g_1 and g_2 exhibit the merging behavior as the system size L increases, indicating the presence of a KT phase transition. At high temperatures, g_1 decreases to zero while g_2 exhibits a negative dip with increasing L. By extrapolating the data to $L \rightarrow \infty$ follow Eq. (6), we estimate the critical temperature $T_c \approx 0.885$. Therefore, in the large Δ region, a single KT phase transition occurs from the disordered phase (P) to the quasi-long-range ferromagnetic phase (F). This observation agrees with previous studies [13, 17]. Indeed, this is a phase transition from the disordered phase, where the spins are set randomly, to the quasi-long-range order, where the spins are aligned both in the sense and orientation. Therefore, both magnetic and nematic Binder parameters are sensitive to this phase transition, explaining the merging behavior of both quantities. One can use the two Binder parameters interchangeably to detect the phase transition.

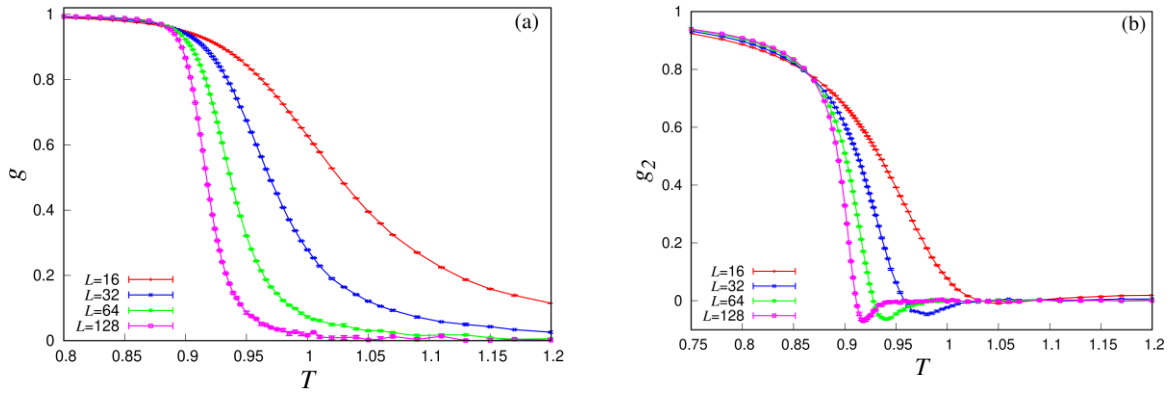

Figure 3. Temperature dependence of the magnetic Binder parameter g_1(a) and the nematic Binder parameter g_2(b) for Δ = 0.7. The error bars are smaller than the symbol sizes.

We focus on the region of the phase diagram where both the nematic and magnetic terms contribute significantly to the physics of the system. This region is specified by Δ away from 0 and 1, and mostly in the range around the tricritical point $\Delta_c \approx 0.325$. The difficulty in this region is that due to the

competition between the nematic and magnetic interactions, the Binder parameter at finite sizes may contain features from the phases below and above Δ_c. Our goal is thus to determine the phase transitions in this region from this mix of features. For that purpose, we investigate the cases $\Delta = 0.3$ and 0.36, which are slightly below and above the tricritical point Δc.

For $\Delta = 0.3$, which is slightly below Δ_c, we found that the behavior of the Binder parameters is qualitatively similar to the case of $\Delta = 0.2$. The magnetic Binder parameter (g_1) shows a crossing behavior at T_1 for the N → F transition, suggesting an Ising phase transition. The nematic Binder parameter (g_2) exhibits a merging behavior at T_2 for the P → N transition, indicating a KT phase transition. These critical temperatures are obtained straightforwardly, and the crossing behavior appears stable in the thermodynamic limit. As a result, for $\Delta < \Delta_c$, the critical temperatures are well-defined. At $\Delta = 0.36$, which is slightly above Δ_c, the nematic phase starts to influence the behavior of the g_2 in Figure 4b. While the g_1 (Figure 4a) still exhibits the crossing behavior with a large change at the critical temperature, the behavior of g_2 is more complex. It shows a merging feature, and based on this, you obtain $T_2 \approx 0.707$, while assuming the crossing behavior for g_1, we find $T_1 \approx 0.709$. Remarkably, T_1 is approximately equal to T_2, which is consistent with previous studies [13, 17]. For Δ slightly above the tricritical point Δ_c, crossing and merging behaviors coexist in the Binder parametes at the same phase transition remains a mysterious nature. It is the reason for devoting the next section to understanding this issue.

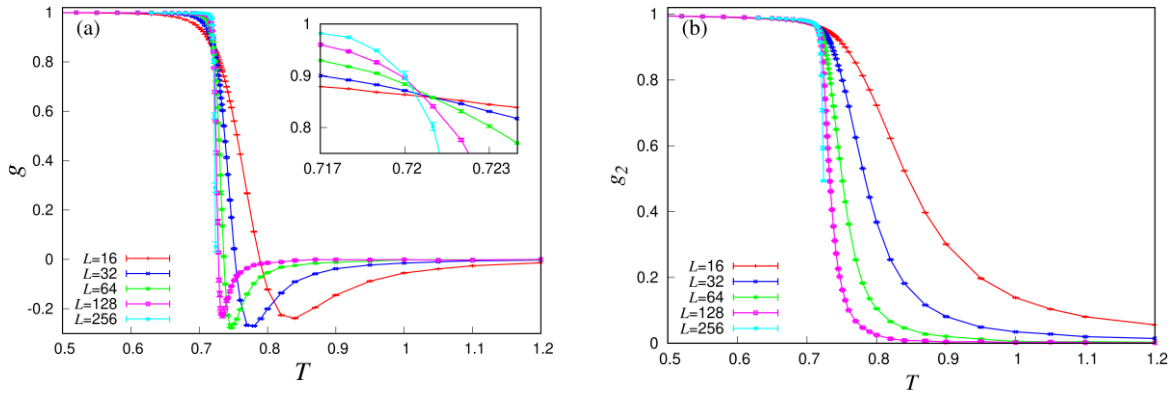

Figure 4. Temperature dependence of the magnetic Binder parameter g_1 (a) and the nematic Binder parameter g_2 (b) for $\Delta = 0.36$. The inset in panel (a) is the expanded view of the magnetic Binder parameter around the crossing temperature. The error bars are smaller than the symbol sizes.

4. Ising and KT Transition Lines

The consensus is that the phase transition from the nematic to the quasi-long-range order below the tricritical point (see Figure 1) belongs to the Ising universality class [9, 13-15]. The remaining open questions focus on the tricritical region: i) Whether this Ising line goes beyond the tricritical point: ii) the nature of the Ising segment beyond the tricritical point if there is; and iii) The transition from the Ising to the KT universality class along this line. Some of these issues have been studied in Refs. 14 and 15, which focus on the modified Villain model of Eq. (1) and claim that the Ising transition line goes beyond the tricritical point. The Monte Carlo study of Ref. 13 directly simulates Eq. (1) but only briefly mentions the possibility of the Ising transition above the tricritical point based on the specific heat measurements. The Monte Carlo simulation of Ref. 17 re-examines Eq. (1), suggesting that the Ising

phase transition terminates at the tricritical point, leading to an intermediate region between the Ising and KT lines based on the correlation length. We hope to support more insights into some of the above questions using the Binder parameter.

First, we note that there is ambiguity if observing directly the Binder parameter. As discussed in Sec. 3, the magnetic Binder parameter expresses a crossing behavior in the region $\Delta \gtrsim \Delta_c$ (e.g., at $\Delta = 0.36$), which may indicate an Ising-like phase transition. However, due to computational limitations, it may be challenging to determine whether this crossing behavior persists, changes to merging behavior, or remains inconclusive in the thermodynamic limit. On the other hand, the nematic Binder parameter clearly shows the merging behavior, a signature of the KT-type transition associated with the binding and unbinding of half-vortices. However, g_2 primarily relates to the pairing of half-vortices, and it may not provide direct evidence regarding the extension of the Ising line beyond the tricritical point.

Second, as discussed in Sec. 3, the magnetic Binder parameter develops a negative dip for a wide range of Δ, which may indicate the system exhibits two phase transitions at T_1 and T_2, respectively. Figure 5 presents the negative depth $h_g(L)$ of the magnetic Binder parameter versus the inverse system size $1/L$ for several values of Δ. For $\Delta > 0.35$, the $h_g(L)$ tends to decrease as L increases, which means that the dip of the magnetic Binder parameter might go up to zero, indicating that the system has only one phase transition. For $\Delta \leq \Delta_c$ and $\Delta_c < \Delta \leq 0.35$, $h_g(L)$ tends to increase as L increases, which means that the magnetic Binder parameter curves have a finite negative dip, suggesting the system has two phase transitions at T_1 and T_2. Therefore, for Δ slightly above the tricritical point Δ_c, the magnetic Binder parameter still shows the coexistence of T_1 and T_2 at the same phase transition.

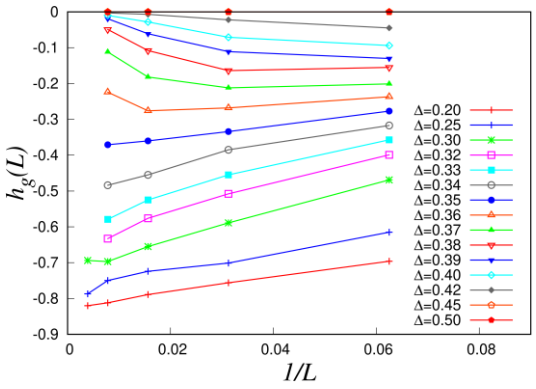

Figure 5. The negative depth of the magnetic Binder parameter as a function of $1/L$ for a wide range of Δ.

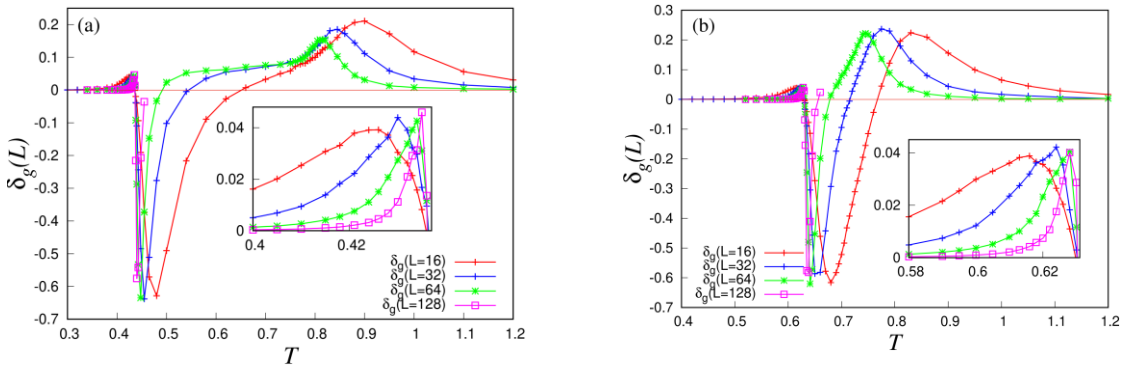

Figure 6. Temperature dependence of the difference of the magnetic Binder parameter $\delta_g(L)$ for $\Delta < \Delta_c \approx 0.325$, particularly at $\Delta = 0.2$ (a) and at $\Delta = 0.3$ (b). Insets are the expanded views of the $\delta_g(L)$ in the region below T_1, where it exhibits peaks with maximal values.

Figure 6 shows the difference of the magnetic Binder parameter $\delta_g(L)$ for $\Delta < \Delta_c$ at $\Delta = 0.2$ (a) and $\Delta = 0.3$ (b). $\delta_g(L)$ exhibits a peak with a maximum value at a temperature below T_1. For $\Delta < \Delta_c$, which is known to exhibit the Ising phase transition. $\delta_g^{max}(L)$ at T_1 does not change significantly as L increases, leading that the crossing behavior of $g_1(L)$ is maintained in the thermodynamic limit. This observation confirms that the phase transition T_1 at $\Delta = 0.2$ and $\Delta = 0.3$ is true of the Ising type.

Figure 7 shows the difference of the magnetic Binder parameter $\delta_g(L)$ for $\Delta > \Delta_c$ at $\Delta = 0.36$ (a) and $\Delta = 0.4$ (b). $\delta_g^{max}(L)$ at T_1 below the crossing temperature systematically decreases as the lattice size L increases. This signal is easily observed even at small lattice sizes, e.g. with L running from 16 to 128, indicating that the crossing behavior of $g_1(L)$ at T_1 tends to disappear in the thermodynamic limit. There are two possible scenarios for the phase transition at $\Delta = 0.36$ and 0.4: (1) If $\delta_g^{max}(L)$ approaches zero as $L \to \infty$, then the crossing behavior of the Binder parameter will change to a merging behavior, suggesting that the phase transition is of KT-type; (2) If $\delta_g^{max}(L)$ reaches a finite value as $L \to \infty$, then the crossing behavior of $g_1(L)$ will be maintained in the thermodynamic limit, suggesting the phase transition is another Ising-type transition, but may have different physics than the N → F transition.

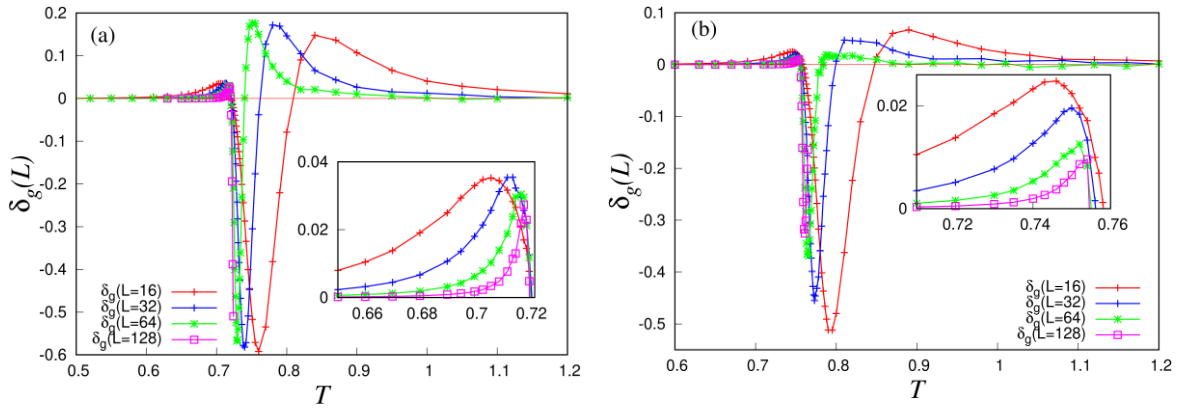

Figure 7. Temperature dependence of the difference of the magnetic Binder parameter $\delta_g(L)$ for $\Delta > \Delta_c \approx 0.325$, particularly at $\Delta = 0.36$ (a) and at $\Delta = 0.4$ (b). Insets are the expanded views of the $\delta_g(L)$ in the region below T_1, where it exhibits peaks with maximal values.

Figure 8 is another view of the difference in the Binder parameter at T_1. It is the plot of $\delta_g^{max}(L)$ versus $1/L$, showing the tendency of the maxima of δ_g at T_1 as L increases. For $\Delta \leq \Delta_c$, the curves are approximately horizontal lines, indicating that the maxima of δ_g remains relatively constant as L increases. This behavior confirms that the phase transition from N → F belongs to the Ising universality class. For $\Delta_c < \Delta < 0.4$, the curves bend at Δ close to Δ_c, requiring larger-scale simulations to understand the physics. However, for $\Delta \geq 0.35$, the curves show a clear tendency toward zero as L increases. For $\Delta \geq 0.4$, the curves become relatively linear and clearly go to zero, thus the merging behavior can occur at large enough L for $\Delta \geq 0.4$, confirming the KT phase transition. Therefore, the range of interest is $\Delta_c < \Delta < 0.4$, and while we cannot access larger-scale simulation, at least for $\Delta \geq 0.35$, we can say that the phase transition is not a conventional Ising-type, as the crossing behavior of the Binder parameter is not maintained in the thermodynamic limit. It is not true of KT type either as $\delta_g^{max}(L)$ goes to zero rather slowly, thus behaving differently from that at $\Delta \geq 0.4$.

$\delta_g(L)$ exhibits a peak with a maximum value at a temperature below T_2 for $\Delta < \Delta_c$ in Figure 6. For $\Delta = 0.2$, $\delta_g^{max}(L)$ at T_2 tends to decrease as L increases, leading to a merging behavior of $g_1(L)$ at a finite value in the thermodynamic limit. This signature supports the existence of a phase transition at T_2. For

$\Delta = 0.3$ near Δ_c, $\delta_g^{max}(L)$ at T_2 does not change significantly as L increases, leading that the crossing behavior of $g_1(L)$ might be finite or divergence, an indicator of the existence of a phase transition at T_2.

$\delta_g(L)$ exhibits a peak with a maximum value at a temperature below T_2 $\Delta > \Delta_c$ in Figure 7. For $\Delta = 0.36$, $\delta_g^{max}(L)$ at T_2 tends to increase as L increases, and $g_1(L)$ remains stable at a finite value or diverges in the thermodynamic limit, suggests the existence of a phase transition at T_2 even for Δ slightly above Δ_c. For $\Delta = 0.4$, $\delta_g^{max}(L)$ at T_2 tends to decrease to zero as L increases, suggesting the phase transition disappearance at T_2.

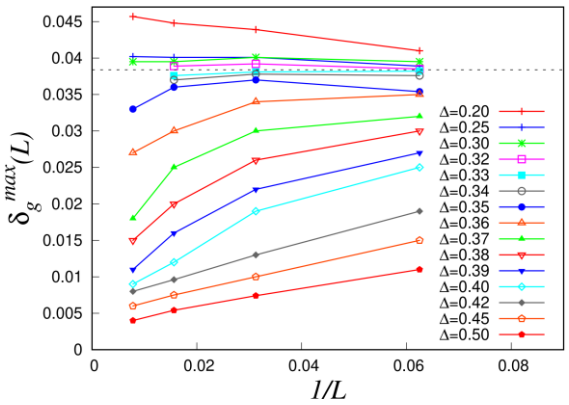

Figure 8. Maximum of $\delta_g(L)$ at T_1 as a function of $1/L$ for a wide range of Δ. The dashed horizontal line separates two regions: $\Delta < \Delta_c$ above the line and $\Delta > \Delta_c$ below the line.

Figure 9 shows $\delta_g^{max}(L)$ at T_2 versus Δ for several system size L=16, 32, and 64. For $\Delta \leq \Delta_c$, $\delta_g^{max}(L)$ at T_2 tends to decrease as L increases, leading to $g_1(L)$ exhibiting a merging behavior at a finite value in the thermodynamic limit, supports the existence of a phase transition at T_2 in this region. For $\Delta_c < \Delta < 0.36$, $\delta_g^{max}(L)$ at T_2 tends to increase as L increases, and $g_1(L)$ remains stable at a finite value or diverges in the thermodynamic limit, supports the presence of a phase transition at T_2. For $0.36 < \Delta < 0.4$, where the system seems to exhibit a transition from Ising-like behavior to KT-like behavior, $\delta_g^{max}(L)$ at T_2 behaves similarly to the $\Delta < \Delta_c$ regime further suggests the existence of a phase transition at T_2. For $\Delta \geq 0.4$, $\delta_g^{max}(L)$ at T_2 decreasing to zero as L increases, suggesting the phase transition disappearance at T_2 in this region. Therefore, the range of interest is $\Delta_c < \Delta < 0.4$, and while we cannot access larger-scale simulation, at least for $\Delta_c < \Delta < 0.36$, we can say that the phase transition is not a conventional Ising-type or KT-type, as the co-existence of T_1 and T_2 at the same temperature.

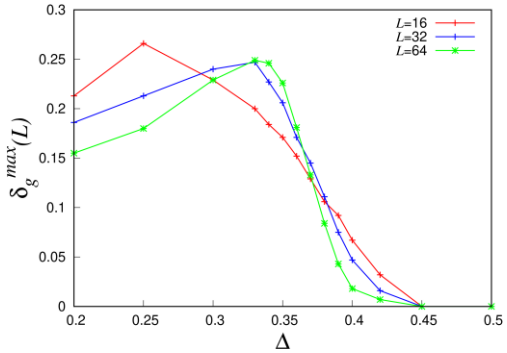

Figure 9. Maximum of $\delta_g(L)$ at T_2 as a function of Δ for several system sizes L. For $\Delta_c < \Delta < 0.36$, the size-dependence of $\delta_g^{max}(L)$ at T_2 behave difference with that in the other region.

Therefore, the region of $\Delta_c < \Delta < 0.4$ is special. It may be related to the region for the "deconfinement phase transition" proposed by Serna et al., [15]. However, the "deconfinement" physics is not clear from the perspective of the Binder parameter. Instead, the Binder parameter can only separate this region from those of the Ising and KT transitions. The upper limit $\Delta \approx 0.4$ is detected by both the Binder parameters, distinguishing it from the usual KT transition at larger Δ, while the lower limit at Δ_c can only be observed using the Binder parameter. However, both $g_1(L)$ at criticality and $\delta_g(L)$ show that this phase transition segment is not a continuation of the Ising line of the N-F transition, which is unable to observe using other quantities such as the specific heat. The nature of the phase transition in this segment differs from that of other regions. It can be considered as the intermediate region connecting the Ising transition line and the KT transition line. Therefore, in the phase diagram, we distinguish it (the yellow square line in Figure 1) from other phase transition lines. It is consistent with previous studies [17].

5. Conclusions

In summary, we have studied the behaviors of the magnetic and nematic Binder parameters g_n in the two-dimensional generalized XY model at $q = 2$. We demonstrated the power of g_n in determining the phase transitions and classifying the type of a phase transition without directly calculating the critical exponents. We used the Binder parameter to reconstruct the phase diagram, consistent with previous studies from other physical quantities. The phase transition in the region $\Delta_c \approx 0.325$ to 0.4 exhibits different physics from those below Δ_c or above 0.4. This intermediate region is between the Ising and KT transition lines, which are characterized by changing behaviors of the Binder parameter from more Ising-like near Δ_c to more KT-like near $\Delta \approx 0.4$.

Acknowledgements

We are grateful to Dr. Dang The Hung for useful discussion. This research is funded by Vietnam National Foundation for Science and Technology Development (NAFOSTED) under Grant No. 103.05-2019.44.

References

[1] N. D. Mermin, H. Wagner, Absence of Ferromagnetism or Antiferromagnetism in One- or Two-Dimensional Isotropic Heisenberg Models, Physical Review Letters, Vol. 17, 1966, pp. 1133-1136, https://doi.org/10.1103/PhysRevLett.17.1133.

[2] V. L. Berezinskii, Destruction of Long-range Order in One-dimensional and Two-dimensional Systems Having a Continuous Symmetry Group I. Classical Systems, Soviet Physics JETP, Vol. 32, 1971, pp. 493-500, http://www.jetp.ras.ru/cgi-bin/e/index/e/32/3/p493?a=list.

[3] J M Kosterlitz, D J Thouless, Ordering, Metastability and Phase Transitions in Two-Dimensional Systems, Journal of Physics C: Solid State Physics, Vol. 6, 1973, pp. 1181-1203, https://doi.org/10.1088/0022-3719/6/7/010.

[4] S. E. Korshunov, Possible Splitting of A Phase Transition in a 2D XY Model, JETP Letters, Vol. 41, 1985, pp. 263-266, http://jetpletters.ru/ps/1444/article_21975.shtml.

[5] D. H. Lee, G. Grinstein, Strings in Two-dimensional Classical XY Models, Physical Review Letters, Vol. 55, 1985, pp. 541-544, https://doi.org/10.1103/PhysRevLett.55.541.

[6] J. Pang, C. D. Muzny, N. A. Clark, String Defects in Freely Suspended Liquid-Crystal Films, Physical Review Letters, Vol. 69, 1992, pp. 2783-2786, https://doi.org/10.1103/PhysRevLett.69.2783.

[7] L. Bonnes, S, Wessel, Half-vortex Unbinding and Ising Transition In Constrained Superfluids, Physical Review B, Vol. 85, 2012, pp. 0945131-0945131, https://doi.org/10.1103/PhysRevB.85.094513.

[8] M. J. Bhaseen, S. Ejima, F. H. L. Essler, H. Fehske, M. Hohenadler, B. D. Simons, Discrete Symmetry Breaking Transitions Between Paired Superfluids, Physical Review A, Vol. 85, 2012, pp. 0336361-03363616, https://doi.org/10.1103/PhysRevA.85.033636.

[9] D. B. Carpenter, J. T. Chalker, The Phase Diagram of A Generalised XY Model, Journal of Physics: Condensed Matter, Vol. 1, 1989, pp. 4907-4912, https://doi.org/10.1088/0953-8984/1/30/004.

[10] F. C. Poderoso, J. J. Arenzon, Y. Levin, New Ordered Phases in a Class of Generalized XY Models, Physical Review Letters, Vol. 106, 2011, pp. 0672021-0672024, https://doi.org/10.1103/PhysRevLett.106.067202.

[11] G. A. Canova, Y. Levin, J. J. Arenzon, Kosterlitz-Thouless and Potts Transitions in A Generalized XY Model, Physical Review E, Vol. 89, 2014, pp. 0121261-0121265, https://doi.org/10.1103/PhysRevE.89.012126.

[12] G. A. Canova, Y. Levin, J. J. Arenzon, Competing Nematic Interactions in A Generalized XY Model in Two and Three Dimensions, Physical Review E, Vol. 94, 2016, pp. 0321401-03214012, https://doi.org/10.1103/PhysRevE.94.032140.

[13] D. M. H¨ubscher, S. Wessel, Stiffness Jump in the Generalized XY Model on the Square Lattice, Phys. Physical Review E, Vol. 87, 2013, pp. 0621121-0621125, https://doi.org/10.1103/PhysRevE.87.062112.

[14] Y. Shi, A. Lamacraft, P. Fendley, B. Pairing, Unusual Criticality in a Generalized XY Model, Physical Review Letters, Vol. 107, 2011, pp. 2406011-2406015, https://doi.org/10.1103/PhysRevLett.107.240601.

[15] P. Serna, J. T. Chalker, P.Fendley, Deconfinement Transitions in a Generalised XY Model, Journal of Physics A: Mathematical and Theoretical, Vol. 50, 2017, pp. 4240031-42400319, https://doi.org/10.1088/1751-8121/aa89a1.

[16] T. Senthil, A. Vishwanath, L. Balents, S. Sachdev, M. P. A. Fisher, Deconfined Quantum Critical Points, Vol. 303, 2004, pp. 1490-1494, https://www.science.org/doi/10.1126/science.1091806.

[17] D. X. Nui, L. Tuan, N. D. T. Kien, P. T. Huy, H. T. Dang, D. X. Viet, Correlation Length In A Generalized Twodimensional XY Model, Physical Review B, Vol. 98, 2018, pp. 1444211-1444219, https://doi.org/10.1103/PhysRevB.98.144421.

[18] V. D. Touchette, P. P. Orth, P. Coleman, P. Chandra, T. C. Lubensky, Emergent Potts Order in a Coupled Hexatic-Nematic XY Model, Physical Review X, Vol. 12, 2022, pp. 0110431-01104322, https://doi.org/10.1103/PhysRevX.12.011043.

[19] D. Loison, Binder's Cumulant for the Kosterlitz-Thouless Transition, Journal of Physics: Condensed Matter, Vol. 11, 1999, pp. 401-406, https://doi.org/10.1088/0953-8984/11/34/101.

[20] M. Hasenbusch, The Binder Cumulant at the Kosterlitz–Thouless Transition, Journal of Statistical Mechanics: Theory and Experiment, Vol. 08, 2008, pp. 080031-0800321, https://doi.org/10.1088/1742-5468/2008/08/P08003.

[21] D. X. Viet, H. Kawamura, Monte Carlo Studies of Chiral and Spin Ordering of the Threedimensional Heisenberg Spin Glass, Physical Review B, Vol. 80, 2009, pp. 0644181-06441820, https://doi.org/10.1103/PhysRevB.80.064418.

[22] L. M. Tuan, T. T. Long, D. X. Nui, P. T. Minh, N. D. T. Kien, D. X. Viet, Binder Ratio in the Two-Dimensional Q-State Clock Model, Physical Review E, Vol. 106, 2022, pp. 0341381-0341388, https://doi.org/10.1103/PhysRevE.106.034138.

[23] U. Wolff, Collective Monte Carlo Updating for Spin Systems, Physical Review Letters, Vol. 62, 1989, pp. 361-364, https://doi.org/10.1103/PhysRevLett.62.361.

[24] J. Imriska, Phase Diagram of a Modified XY Model, Bachelor's Thesis, Comenius University in Bratislava, 2009.

[25] T. Surungan, Y. Okabe, Kosterlitz Thouless Transition in Planar Spin Models with Bond Dilution, Physical Review B, Vol. 71, 2005, pp. 1844381-1844387, https://doi.org/10.1103/PhysRevB.71.184438.